

Collisionless Dissipative Nonlinear Alfvén Waves: Nonlinear Steepening, Compressible Turbulence, and Particle Trapping *

M.V. Medvedev †

Harvard-Smithsonian Center for Astrophysics, 60 Garden St., Cambridge, MA 02138

The magnetic energy of nonlinear Alfvén waves in compressible plasmas may be ponderomotively coupled only to ion-acoustic quasi-modes which modulate the wave phase velocity and cause wave-front steepening. In the collisionless plasma with $\beta \neq 0$, the dynamics of nonlinear Alfvén wave is also affected by the resonant particle-wave interactions. Upon relatively rapid evolution (compared to the particle bounce time), the quasi-stationary wave structures, identical to the so called (Alfvénic) Rotational Discontinuities, form, the emergence and dynamics of which has not been previously understood. Collisionless (Landau) dissipation of nonlinear Alfvén waves is also a plausible and natural mechanism of the solar wind heating. Considering a strong, compressible, Alfvénic turbulence as an ensemble of randomly interacting Alfvénic discontinuities and nonlinear waves, it is shown that there exist two distinct phases of turbulence. What phase realizes depends on whether this collisionless damping is strong enough to provide adequate energy sink at all scales and, thus, to support a steady-state cascade of the wave energy. In long-time asymptotics, however, the particle distribution function is affected by the wave magnetic fields. In this regime of nonlinear Landau damping, resonant particles are trapped in the quasi-stationary Alfvénic discontinuities, giving rise to a formation of a plateau on the distribution function and quenching collisionless damping. Using the virial theorem for trapped particles, it is analytically demonstrated that their effect on the nonlinear dynamics of such discontinuities is non-trivial and forces a significant departure of the theory from the conventional paradigm.

PACS numbers: 52.35.Mw, 52.35.Ra, 96.50.Bh, 96.50.Ci

I. INTRODUCTION

Alfvén waves are the most ‘robust’ plasma oscillations in magnetized systems. They are encountered in a wide variety of astrophysical objects such as stellar and solar winds, interstellar medium, hot accretion flows, magne-

tospheres of planets and magnetized stars, etc.. It is interesting that in incompressible plasma, $\nabla \cdot \mathbf{v} = 0$, fluid and magnetic nonlinearities in a finite-amplitude Alfvén wave cancel each other exactly, so that it obeys the same dispersion relation as the linear wave of infinitesimal amplitude.

Such a mutual cancellation of Reynolds and magnetic stresses in the wave breaks down when plasma is compressible. Indeed, the magnetic field pressure, $\tilde{B}^2/8\pi$, associated with the wave field ponderomotively modulates the local plasma density, n , which, in turn, affects the phase velocity of the wave. This process may also be viewed as an effective parametric coupling of an Alfvén wave to acoustic waves in plasma. Such acoustic modes, however, are *not* plasma eigenmodes. They are driven by the Alfvén wave and, hence, propagate with the Alfvén speed, which is, in general, different from the sound speed in plasma. The nonlinear coupling of the phase speed of the wave to its amplitude in the *nonlinear Alfvén waves* is ultimately responsible for the wave-front steepening and formation of collisionless shocks in astrophysical and space plasmas.

In studies of nonlinear waves it is customary to assume ‘weak nonlinearity’, i.e., the wave amplitude is finite but still small compared to the ambient field. This means that a wave is linear in the leading order of expansion in wave amplitude. All nonlinear effects appear as a gradual, large-scale modulation of the wave amplitude. In other words, one studies slow evolution of an envelope of a wave packet.

It is well known that in collisionless, *incompressible* plasma, low-frequency Alfvén waves are undamped or very weakly damped since collisionless dissipation is inefficient. Ion-cyclotron damping is always weak for low-frequency waves and Landau damping, which could be important, is absent because there are no longitudinal electric and magnetic field perturbations in the Alfvén wave. Equivalently, an Alfvén wave is strictly transverse in the drift approximation and thus cannot affect the particle motions along the field lines. (Note that weak Landau dissipation of obliquely propagating Alfvén waves occurs on scales comparable to the ion Larmor radius, ρ_i , where the drift approximation breaks down. This damping is really weak since typically $k_{\perp}\rho_i \ll 1$.)

In contrast, a nonlinear Alfvén wave in compressible plasma is nonlinearly coupled to acoustic-type oscillations which are accompanied (in a two-fluid model) by longitudinal electric fields and *are* damped via the Lan-

*Invited talk on the American Physical Society, Division of Plasma Physics meeting, 1998. In collaboration with P.H. Diamond, V.I. Shevchenko, M.N. Rosenbluth, and V.L. Galinsky (UCSD).

†Also at the Institute for Nuclear Fusion, RRC “Kurchatov Institute”, Moscow 123182, Russia;
E-mail: mmedvedev@cfa.harvard.edu; URL: <http://cfa-www.harvard.edu/~mmedvedev/>

dau mechanism. Hence, dissipation enters the dynamics of nonlinear Alfvén waves nonlinearly, even in the regime when the resonant particle response is calculated in the linear approximation, i.e., neglecting trapping of resonant particles. Another important and quite unusual feature is the *nonlocality* of the damping. It is associated with the finite transit time of a resonant particle through the wave envelope modulation and represented by an integral operator in the wave evolution equation.

Unusual properties of dissipation in the nonlinear Alfvén waves naturally result in the following peculiar features of these waves. First of all, it was shown that Alfvén waves do not always damp to zero. Instead, they evolve into the localized, coherent, *quasi-stationary* structures referred to as *directional* and *rotational discontinuities*. These are the narrow regions where the wave magnetic field vector rapidly rotates through some angle and, respectively, are or are not accompanied by the wave amplitude variations. These discontinuities connect the parts of a wave packet of different polarizations or wave phases. Second, among the Alfvénic discontinuities, there are solutions which constitute a new class of shock waves, — the *collisionless dissipative shocks*. Such shocks form when nonlinear wave steepening is balanced by collisionless damping process (and not by the wave dispersion, as in usual collisionless shocks). Due to scale invariance of Landau damping, the shock width is determined by dispersion, however, which is the only characteristic scale in the problem. It should be emphasized that Alfvénic rotational discontinuities have been discovered by *in situ* measurements [1–3] of magnetic fields in the solar wind. Despite intense observational and theoretical efforts these years, a comprehensive quantitative theory which explains the emergence and dynamics of Alfvénic discontinuities was proposed only recently [4–6]. All the results are in excellent agreement with the observational data and numerical hybrid simulations [7,8]. Third, preliminary study of a one-dimensional model of strong, compressible Alfvénic turbulence [9] suggests the existence of two distinct phases or states of the turbulence, depending on how strong the collisionless damping is. At last, resonant particles, which were responsible for the wave damping in the linear Landau process, appear to be trapped in the wave potential at large times and the linear theory of Landau damping is invalid. Qualitatively, the damping rate oscillates with roughly the bounce frequency and gradually decreases to zero until resonant particles phase mix and form a plateau on the distribution function. A recently proposed asymptotic theory of particle trapping [10] predicts non-trivial nonlinear contributions of resonant particles to nonlinear Alfvén wave dynamics. They are the following. (1) The power of the KNLS nonlinearity associated with resonant particles increases to *fourth* order when trapped particles are accounted for. (2) The effective coupling is now proportional to the *curvature* of the particle distribution

function (PDF) at the resonant velocity, $f_0''(v_A)$, and not to its slope, $f_0'(v_A)$, as in linear theory. (3) The *phase-space density* of trapped particles is controlled by plasma β . Thus, the structure of quasi-stationary Alfvénic solitons and discontinuities may be modified in $\tau \rightarrow \infty$ limit.

The rest of this paper is organized as follows. In Sec. II a semi-qualitative derivation of the envelope evolution equation for finite-amplitude Alfvén waves, referred to as the Derivative Nonlinear Schrödinger (DNLS) equation, wave is presented. In Sec. III we generalize it to include the resonant particles effect (Landau damping) and obtain the kinetically modified derivative nonlinear Schrödinger equation (KNLS). We discuss numerical solutions for this equation which appear to be the *Alfvénic Rotational Discontinuities* that observed *in situ* in the solar wind. We also discuss the energy dissipation time scales for various types of nonlinear Alfvén waves. In Sec. IV the noisy-KNLS model of strong, compressible magnetohydrodynamic (MHD) Alfvénic turbulence is discussed. In Sec. V a self-consistent treatment of the nonperturbative effects of particle response (particle trapping) on the nonlinear Alfvén wave dynamics is presented.

II. NONLINEAR ALFVÉN WAVES: THE DNLS EQUATION

The usual derivation of the evolution equation of the nonlinear Alfvén waves is based on the multiple time scale expansion. It assumes that the envelope of an Alfvén wave varies on much longer time-scale, $\tau = (B_0/\tilde{B}_\perp)^2 t \gg t$, than the linear wave period, $t = \omega^{-1} = (k_\parallel v_A)^{-1}$, where B_0 and \tilde{B} are the unperturbed magnetic field and its perturbations, $v_A = B_0/\sqrt{4\pi m_i n}$ is the Alfvén speed, m_i is the ion mass, and \parallel and \perp designate components parallel and perpendicular to the ambient (unperturbed) magnetic field. Such a derivation has been performed by different authors and we refer the reader to the original literature [11,12]. To provide physical insights, we give here a transparent, semi-qualitative derivation instead.

A wave equation of a small amplitude Alfvén wave may be written as

$$(\omega - k_\parallel v_A [1 \pm k_\parallel v_A/2\Omega_i]) \tilde{B}_\perp = 0, \quad (1)$$

where $\Omega_i = eB_0/m_i c$ is the ion-cyclotron frequency. The last term is simply weak dispersion, $k_\parallel v_A/\Omega_i \ll 1$, due to a finite Larmor radius. A ponderomotive force creates density fluctuations, δn , so that the Alfvén speed is no longer constant:

$$v_A = \frac{B_0}{\sqrt{4\pi m_i (n_0 + \delta n)}} \simeq v_{A0} \left(1 - \frac{1}{2} \frac{\delta n}{n_0}\right). \quad (2)$$

We assume that the wave propagates along the magnetic field in z -direction (to the right) and its amplitude is changing gradually, $\tilde{B}_\perp = \tilde{B}_\perp(z - v_{A0}t, \tau)$. Going back

to real-space representation, this suggests the following replacement:

$$\omega \rightarrow -iv_{A0} \frac{\partial}{\partial z} + i \frac{\partial}{\partial \tau}, \quad k_{\parallel} \rightarrow -i \frac{\partial}{\partial z}. \quad (3)$$

We can neglect the variation of v_A in the small dispersion term as a next order effect. From Eq. (1) it is easy to write:

$$\frac{\partial}{\partial \tau} \tilde{B}_{\perp} - \frac{v_A}{2} \frac{\partial}{\partial z} \left(\frac{\delta n}{n_0} \tilde{B}_{\perp} \right) \pm i \frac{v_A^2}{2\Omega_i} \frac{\partial^2}{\partial z^2} \tilde{B}_{\perp} = 0. \quad (4)$$

Hereafter we omit subscript “0” in v_A . The perturbed magnetic field here is a complex quantity and is defined as $\tilde{B}_{\perp} = \tilde{B}_x \pm i\tilde{B}_y$. The density perturbations are caused by the ponderomotive force exerted on plasma by the fluctuating magnetic field of the wave. They are obtained from the continuity, momentum balance equations, and equation of state which yield the equation for ion-acoustic waves with source:

$$\left(\frac{\partial^2}{\partial t^2} - c_s^2 \frac{\partial^2}{\partial z^2} \right) \frac{\delta n}{n_0} = -\frac{v_A^2}{2} \frac{\partial^2}{\partial z^2} \frac{|\tilde{B}_{\perp}|^2}{B_0^2}, \quad (5)$$

where $c_s^2 = \gamma(T_e + T_i)/m_i$ is the ion-acoustic speed, $\gamma = 3$ is the polytropic constant, and $p = n(T_e + T_i)$ and $m_e \ll m_i$ were used in derivation. Since, ion-acoustic waves are driven by the Alfvén wave, the density perturbation is a function of $z - v_A t$. Thus $\frac{\partial^2}{\partial t^2} \equiv v_A^2 \frac{\partial^2}{\partial z^2}$ and Eq. (5) yields:

$$\frac{\delta n}{n_0} = -\frac{1}{2(1-\beta)} \frac{|\tilde{B}_{\perp}|^2}{B_0^2}, \quad (6)$$

where $\beta = c_s^2/v_A^2$ is roughly the ratio of plasma pressure to magnetic pressure. Substituting the density perturbation into the equation for the wave magnetic field (4) and defining $b = \tilde{B}_{\perp}/B_0$, we obtain the DNLS equation:

$$\frac{\partial b}{\partial \tau} + \frac{1}{4(1-\beta)} \frac{\partial}{\partial z} (|b|^2 b) \pm i \frac{v_A^2}{2\Omega_i} \frac{\partial^2 b}{\partial z^2} = 0. \quad (7)$$

This equation describes evolution of planar nonlinear Alfvén waves propagating in one dimension along the ambient magnetic field. It was shown that this equation is solvable [13] and admits soliton and cnoidal wave solutions.

A numerical solution of the initial value problem for the DNLS is shown in Fig. 1a. It is natural to assume that nonlinear waves emerge from small-amplitude (linear) ones. Thus the most general class of initial profiles are the finite-amplitude, periodic waves of different helicities (polarizations). In the case of Fig. 1a, an initially linearly polarized, sinusoidal initial wave profile has been chosen. (The range of dimensionless coordinate, $0 \leq \zeta \leq 1024$ corresponds to the number harmonics used in calculation, $-512 \leq k \leq 512$.) One can see that wave front indeed steepens at early times, $\tau \sim 2 \sim 400\Omega_i^{-1}$.

Later, at $\tau \sim 5$, when the width of the front becomes of order Ω_i/v_A dispersion limits nonlinear steepening and produces small-scale, oscillatory wave-like structures with significant small-scale energy component. At later times, the magnetic field is highly irregular indicating strong nonlinear Alfvén wave turbulence. Note that *no (quasi-stationary) Alfvénic discontinuities emerge*.

III. NONLINEAR ALFVÉN WAVES WITH LANDAU-TYPE DISSIPATION: THE KNLS EQUATION

It is known that kinetic effects like Landau damping are absent from the MHD approximation. To include them into the nonlinear Alfvén wave model self-consistently, a fully kinetic treatment is needed [14]. The results are often too complicated and obscuring, however. There are two ways to go around the difficulties. First way is to use a hybrid MHD-kinetic approach in which one performs the *ad hoc* calculations the quantities which are known to be affected by kinetics (i.e., the density perturbations, δn) and plugs them into the MHD model [15–17]. Second way is to make some self-consistent closures in deriving the MHD equations to modify them so that to mimic collisionless processes [18]. Then these new MHD equations may be used to re-derive the nonlinear Alfvén wave equation [5]. Here we again give a simple, semi-qualitative derivation. For rigorous analysis, we refer reader to the original literature [5,15–17].

To include kinetic effects, we need to modify the equation for ion-acoustic waves only, while Eq. (4) remains unchanged. The equation of damped ion-acoustic modes may be formally written as

$$\left(\frac{\partial^2}{\partial t^2} + \hat{\gamma} \frac{\partial}{\partial t} - c_s^2 \frac{\partial^2}{\partial z^2} \right) \frac{\delta n}{n_0} = -\frac{v_A^2}{2} \frac{\partial^2}{\partial z^2} \frac{|\tilde{B}_{\perp}|^2}{B_0^2}, \quad (8)$$

where $\hat{\gamma}$ is a damping rate. If the damping rate is a function of k in Fourier space, $\hat{\gamma}$ in real space is represented by an operator acting on a wave field. We now recall that in k -space Landau damping rate is proportional to $1/|k_{\parallel}|$. Thus in real space we write

$$\hat{\gamma} = v_A \chi \hat{\mathcal{H}} \frac{\partial}{\partial z}, \quad (9)$$

where $\hat{\mathcal{H}}[f] = \frac{1}{\pi} \int_{-\infty}^{\infty} \frac{\mathcal{P}}{z' - z} f(z') dz'$ is the integral Hilbert operator acting on a function f (\mathcal{P} denotes principal value integration), which is equal to $(ik_{\parallel}/|k_{\parallel}|)f_k$ in Fourier space and, thus, ensures correct k -scaling of collisionless damping. Here χ is a parameter which contains all insignificant physics such as the structure of a PDF, etc., and depends on the closure chosen. In the model of Ref. [5], χ has the physical meaning of a thermoconductivity coefficient. Again, we assume a traveling wave

solution for the density perturbations, $\delta n = \delta n(z - v_A t)$. Then we have

$$(1 - \beta) \frac{\delta n}{n_0} + \chi \hat{\mathcal{H}} \left[\frac{\delta n}{n_0} \right] = -\frac{1}{2} |b|^2. \quad (10)$$

To solve this equation we use the identity $\hat{\mathcal{H}}\hat{\mathcal{H}} = -1$, which has a physical meaning of *time-reversibility* of Landau damping [5]. Acting on Eq. (10) with $\hat{\mathcal{H}}$, excluding $\hat{\mathcal{H}}[\delta n/n_0]$ and substituting into Eq. (4), we obtain the KNLS equation:

$$\frac{\partial b}{\partial \tau} + v_A \frac{\partial}{\partial z} \left(m_1 b |b|^2 + m_2 b \hat{\mathcal{H}}[|b|^2] \right) + i \frac{v_A^2}{2\Omega_i} \frac{\partial^2 b}{\partial z^2} = 0, \quad (11)$$

where $m_1 = (1 - \beta)/4\Delta$, $m_2 = -\chi/4\Delta$, $\Delta = (1 - \beta)^2 + \chi^2$, are coefficients, which are model-dependent. The rigorous derivation [5] yields

$$m_1 = \frac{1}{4} \frac{(1 - \beta^*) + \chi^2(1 - \beta^*/\gamma)}{(1 - \beta^*)^2 + \chi^2(1 - \beta^*/\gamma)^2}, \quad (12a)$$

$$m_2 = -\frac{1}{4} \frac{\chi\beta^*(\gamma - 1)/\gamma}{(1 - \beta^*)^2 + \chi^2(1 - \beta^*/\gamma)^2}, \quad (12b)$$

where $\beta^2 = (T_e + T_i)\beta/T_i \simeq (T_e/T_i)\beta$ for $T_i \lesssim T_e$, and χ is the best fit parameter of the closure to the exact kinetic particle response [18] with a temperature correction, $\chi = \sqrt{8\beta/\pi\gamma} \exp\{-1/\beta\} (T_e/T_i)^{3/2} \exp\{(T_i - T_e)/2T_i\}$. The dependence of m_1 and m_2 vs. $1/\beta$ is drawn in Fig. 2. Negative sign of m_2 indicates damping. The damping of an Alfvén wave is strongest in warm, isothermal plasmas, $\beta \sim 1$, $T_e \sim T_i$. The KNLS equation straightforwardly generalizes to the case of obliquely propagating waves. In fact, Eq. (11) remains unchanged, but the wave field is re-defined as follows: $b = (\hat{B}_x + i\hat{B}_y + B_0 \sin \Theta)/B_0$, where Θ is the obliquity angle, $\sin \Theta \propto \mathbf{k} \cdot \mathbf{B}_0$.

Clearly, m_1 and m_2 are functions of T_e/T_i and β . It can be shown that if either $T_e/T_i \gg 1$, or $\beta \gg 1$, or $\beta \ll 1$, the Landau damping of nonlinear Alfvén waves becomes very weak, $m_2 \rightarrow 0$. Then the DNLS nonlinearity dominates and $m_1 \rightarrow (1 - \beta)^{-1}$, i.e., changes sign at $\beta \simeq 1$. In this regime, other dissipation mechanisms (e.g., ion-cyclotron damping of the linear Alfvén wave [carrier]) may become important, see Sec. III B.

A. Alfvénic discontinuities

The KNLS equation (11) reduces to the DNLS for $\beta \rightarrow 0$. Collisionless damping of nonlinear Alfvén waves vanishes in this case. The wave dynamics is thus decoupled from resonant particle effects and Alfvénic discontinuities do not emerge (unless one artificially plugs in diffusion, finite plasma conduction, or other collisional effects, as done in some simulations). For finite β 's, the

nonlinear Alfvén wave evolution is affected by resonant particles and is described by the second nonlinear, integral term in Eq. (11). Unlike the DNLS equation, the KNLS equation is not integrable because of dissipation. Numerical solution of this integro-differential equation for the same initial conditions as in Fig. 1a and $\beta = 1$, reveals different wave dynamics, as shown in Fig. 1b. Instead of irregular, fluctuating wave fields, localized, quasi-stationary waveforms (Alfvénic discontinuities) are seen to form very rapidly, within $\tau \lesssim 5 = 10^3 \Omega_i^{-1}$. There are three parameters (in addition to β and T_e/T_i) which control the wave dynamics as well as specify the type of discontinuity which results. These are (i) the wave helicity (i.e., the polarization type), (ii) the obliquity angle Θ , and the angle between the polarization plane (for nearly linear polarizations) and \mathbf{k} - \mathbf{B}_0 plane.

There are three general types of *quasi-stationary* Alfvénic discontinuities, discriminated by the obliquity and phase jump (i.e., angle through which the magnetic field vector rotates). First, there is a wide class of the *arc-type* rotational discontinuities which emerge in *oblique* propagation, $\Theta \gtrsim 10^\circ$, independent of the wave helicity (polarization). They are characterized by an arc-type shape diagram in the hodograph (the b_x - b_y diagram), as shown in the “snap-shot”, Fig. 3. The wave phase jump through the discontinuity is $\Delta\phi < \pi$. Second, there is a class of the *S-type* directional discontinuities which emerge in *quasi-parallel* propagation, $\Theta \sim 0^\circ$, only from linearly and almost linearly polarized initial perturbations. They are characterized by a remarkable S-shaped hodograph, as shown in Fig. 4. They are called directional (not rotational) discontinuities because the phase jump is accompanied by moderate amplitude variation. The wave phase changes by $\Delta\phi = \pi$ through the discontinuity. Third, there is a narrow class of arc-type rotational discontinuities propagating parallel to the magnetic field. They emerge from waves with elliptical polarization only. The wave phase change is $\Delta\phi = \pi$. Parallel propagating circularly polarized waves (helicity equals to unity) do not evolve to discontinuities and are decoupled from dissipation.

B. Comparison with observations

There are two regimes of the Alfvén wave evolution, depending on the values of T_e/T_i and β . Although there is no sharp boundary between the regimes, a *qualitative* insight may be gained from Fig. 6, where the curve $|m_1| = |m_2|$ is plotted. Kinetic damping is important for T_e/T_i and β from the region labeled “hydrodynamic”. There $|m_1| < |m_2|$ and Alfvénic rotational discontinuities rapidly form. We emphasize the remarkably good correspondence of the KNLS solutions and the solar wind observational data [1–3]. Recent $2\frac{1}{2}$ hybrid code simulations are also in excellent agreement with the results of

the KNLS theory [7,8] and thus support the idea that the mechanism of formation of Alfvénic discontinuities is the combined effect of resonant wave-particle interactions and nonlinear wave steepening.

In the opposite case, $|m_1| \gg |m_2|$ (labeled “bursty” in Fig. 6), the Landau damping is weak and may be neglected compared to the ion-cyclotron one. Nonlinear wave steepening cascades wave energy to the scales $k \sim \max\{|m_1|, |m_2|\} |b|^2 \Omega_i / v_A$, as estimated from Eq. (11). Thus, the number of particles being in the cyclotron resonance, $k(v_A - v) - \Omega_i = 0$, may be large if $m_2 \rightarrow 0$, $\beta \simeq 1$. Nonlinear dynamics in this case is governed by the so called DNLS-Burgers equation [19]. This theory explains well the emergence and evolution of Alfvén shock trains (also referred to as “shocklets”) [20], which were observed upstream of the bow-shocks of planets and comets (see e.g., Ref. [21]).

C. Energy dissipation

Resonant particle effects make the otherwise almost non-dissipative Alfvén waves to damp. Fig. 5 shows temporal evolution of magnetic energy associated with different structures (Alfvénic discontinuities). Clearly, the energy dissipation rate in the case of quasi-parallel propagation is sensitive to the initial polarization, i.e., helicity, which is, roughly, a measure of asymmetry of a spectrum between $+k$ and $-k$ harmonics. Crude estimates [6] of the typical damping time are: (i) for linearly polarized waves (zero helicity), e.g., the S-type discontinuities, $\tau_{\text{lin}} \propto |m_2|^{-1}$ and the damping is algebraic, $|b|^2 \propto \tau^{-1/2}$, rather than exponential, (ii) for elliptically polarized waves $\tau_{\text{ell}} \propto |m_2 \Delta_s|^{-1}$, where $\Delta_s \sim \sum (|b_{+k}|^2 - |b_{-k}|^2)$ is a measure of spectrum asymmetry, and (iii) for circularly polarized waves (helicity unity) $\tau_{\text{cir}} \rightarrow \infty$ as they do not damp. In the case of oblique propagation, the ambient field enters the damping rate and for all wave helicities $\tau_{\text{obl}} \propto |m_2 \sin^2 \Theta|^{-1}$. From Fig. 5 one sees that the a typical time-scale of the wave damping is $\tau \lesssim 100 \sim 10^4 \Omega_i^{-1}$, which is (roughly) a few hours for the solar wind conditions.

Given the spectrum of magnetic field energy perturbations, $E_k = (|b|^2)_k$, the instantaneous rate of energy change is calculated *exactly* [6,24] from Eq. (11) to yield:

$$\frac{\partial E}{\partial \tau} = m_2 \int_{-\infty}^{\infty} |E_{k_{\parallel}}|^2 |k_{\parallel}| dk_{\parallel}. \quad (13)$$

Note that this equation is equally applicable to the single wave case as well as to the compressible Alfvénic turbulence in general, provided the turbulence spectrum is known.

Typical dissipation timescale is several hours for the solar wind conditions. Hence, collisionless dissipation of

nonlinear Alfvén waves a plausible (and natural) mechanism of the solar wind heating within one astronomical unit.

IV. COMPRESSIBLE TURBULENCE OF NONLINEAR ALFVÉN WAVES

There are two approaches in the studies of turbulence, cascade and structure-based. The cascade-type theories usually treat turbulence as a “soup of eddies”, — a collection of plasma excitations with random phases which interact with each other (usually on matching scales) and produce a cascade of energy. The structure-based-type approach, one of the examples of which is the noisy Burgers model in hydrodynamics, is based on the study of nonlinear evolution equations with external noise drive. It thus studies the turbulence of coherent structures, such as shocks, solitons, nonlinear (cnoidal) waves, etc., generated and interacting with each other randomly. Such a process may be referred to as “coherent cascade”, meaning that modes (eddies) at all scales interact coherently (in phase) and, thus, experience stronger interactions due to the cumulative effect. It is known that the first approach is more suitable for studies of weak turbulence and the second one better describes the strong, highly nonlinear turbulence.

The analytical study of the structure-based noisy-KNLS model as a generic model of collisionless, large-amplitude, compressible MHD (Alfvénic) turbulence is presented in Ref. [9]. Stationarity is maintained via the balance of noise and dissipative nonlinearity. The Fourier-transformed KNLS equation (11) with noise source reads

$$(-i\omega + iv_0 k + i\mu_0 k^2) b_{\omega}^k + i\lambda k \sum_{\substack{k', k'' \\ \omega', \omega''}} b_{\omega'}^{k'} b_{\omega''}^{k''} b_{\omega - \omega' - \omega''}^{k - k' - k''} \times [m_1 + im_2 \text{sgn}(k - k')] = f_{\omega}^k, \quad (14)$$

where v_0 and μ_0 are the bare phase velocity (it is necessary for a self-consistent renormalization analysis) and dispersion, $\lambda = 1$ is the standard perturbation parameter, and the function $\text{sgn}(x) = x/|x|$. Here we omitted the subscript \parallel by k . The one loop renormalization group analysis of the problem with zero mean, δ -correlated noise with white k -spectrum yields complex-valued renormalized coefficients v_{turb} , μ_{turb} . The ‘Re’ and ‘Im’ parts of μ_{turb} are simply turbulent dispersion and turbulent viscosity. The real part of v_{turb} may be interpreted as wave momentum loss via interactions with resonant particles and its imaginary part manifests fast, exponential damping due to phase mixing. Further analysis shows the existence of two different phases of turbulence. The bifurcation occurs at the point

$$|m_1/m_2| \simeq 1. \quad (15)$$

If $|m_1/m_2| < 1$, Landau dissipation is efficient to sink all the injected energy during the “coherent cascade” so that the hydrodynamic ($\omega \rightarrow 0$, $k \rightarrow 0$) regime with no sharp fronts realizes. In this regime, the strongly interacting Alfvénic discontinuities dominate in the turbulence. In the opposite case, nonlinearity overcomes damping and no stationary, hydrodynamic turbulence is predicted. Small-scale, bursty turbulence is expected in this regime. Given the weak cyclotron damping, such a regime corresponds to the Alfvénic shocklet turbulence. Recalling that m_1 and m_2 are functions of β and T_e/T_i , a “diagram of state” can be drawn, as shown in Fig. 6.

V. ASYMPTOTIC, $\tau \rightarrow \infty$, DYNAMICS OF DISSIPATIVE NONLINEAR ALFVÉN WAVES

The linear Landau damping theory used in derivation of the KNLS assumes a time-independent (Maxwellian) PDF. It is clear that, for a finite-amplitude wave, particles which are near resonance with the wave, $v \simeq v_A$, will be trapped by the wave potential $U(z) \equiv \tilde{B}_\perp^2/8\pi n_0$ because their kinetic energy (measured in the wave frame), $\frac{1}{2}m(v - v_A)^2$, is less than the potential barrier, $|U_m| = \max|U(z)|$, as in Fig. 7. Such particles experience reflections at turning points z_1 and z_2 exchanging energy with the wave and significantly modify the PDF near resonance. The damping rate of a wave oscillates in time with gradually decreasing amplitude until phase mixing results in flattening of the PDF (for resonant velocities) and formation of a *plateau*; then the damping rate vanishes [22]. Thus, the *linear* calculation of Landau dissipation, while correct for times short compared to the typical bounce (trapping) time, $\tau \ll \tau_{tr} \simeq (k_\parallel \sqrt{U/m_i})^{-1} \simeq (k_\parallel v_A |b|)^{-1}$, fails for quasi-stationary waveforms (Alfvénic discontinuities) on times $\tau \gtrsim \tau_{NL} \gg \tau_{tr}$ [$\tau_{NL}^{-1} \simeq m_1 k_\parallel v_A (\tilde{B}_\perp^2/B_0^2)$ is the typical nonlinear wave profile evolution time]. Hence, Landau dissipation should be calculated *non-perturbatively* to determine the resonant particle response to the nonlinear wave.

The nonlinear Landau damping problem is, in general, not *analytically* tractable, as it requires explicit expressions for *all* particle trajectories as a function of initial position and time. Such trajectories cannot be explicitly calculated for a potential of *arbitrary shape*. Usually, a full particle simulation is required. In some cases, it is useful to approximate the wave profile shape by a simple analytic expression which may be assumed to persist, while the wave amplitude varies, to calculate the trajectories [23]. This is not the case for our problem because nonlinear Landau damping controls the profile of the Alfvén wave.

A nonperturbative, self-consistent theory of nonlinear wave-particle interactions was constructed in the asymptotic limit, $\tau \rightarrow \infty$, applying the virial theorem to deter-

mine the PDF. The generalized KNLS again is Eq. (4) with $\delta n = \delta n_{NR} + \delta n_R$, where δn_{NR} and $\delta n_R \propto \chi \hat{\mathcal{K}}[U(z)]$ are the non-resonant (bulk) and resonant particle responses, respectively. Here $\hat{\mathcal{K}}$ is a new kinetic operator (which replaces $\hat{\mathcal{H}}$) acting of the wave field which contains all the information about resonant (trapped) particle trajectories. It is interesting that the very possibility of writing the generalized KNLS equation in this form relies on the intrinsic *time reversibility* of the Vlasov equation, linear or nonlinear: $\hat{\mathcal{K}}\hat{\mathcal{K}} = -1$, see Ref. [5].

The resonant particle response is calculated using *Liouville’s theorem* (“the PDF is constant along particle trajectories”):

$$f(v, z, t) = f_0(v_\pm(E, z_0^\pm)), \quad (16)$$

where $z_0^\pm = z_0^\pm(z, t, E; U(z))$ is the *initial* coordinate of a particle of total energy E which at time t is at the point z and has a velocity $v_\pm(E, z)$. By definition $\delta n_R = \int_{\Delta v_{res}} dv (f - f_0^{(t=0)})$, so that

$$\delta n_R = \sum_{(\pm)} \int_{\Delta E_{res}} \frac{f_0(v_\pm(E, z_0^\pm)) - f_0(v_\pm(E, z))}{\sqrt{2m_i(E - U(z))}} dE. \quad (17)$$

Here the sum is over particles moving to the right (+) and to the left (−), as in Fig. 7. The integration is over the resonant (negative) energies of trapped particles, $U_m \leq E \leq 0$ with U_m being the amplitude of the potential. In the short-time limit, $\tau \rightarrow \infty$, Eq. (17) reduces to the KNLS case with $\hat{\mathcal{K}} = \hat{\mathcal{H}}$ and $\chi = \pi v_A^2 f_0'(v_A)/m_i n_0$.

To treat the $\tau \rightarrow \infty$ limit we employ the *virial theorem*, which relates the average kinetic and potential energies of particles trapped in an adiabatically changing potential:

$$2\langle K(z) \rangle = n\langle \tilde{U}(z) \rangle. \quad (18)$$

Here $\tilde{U}(z) = U(z) - U_m$ is a *homogeneous* function of its argument of order n , i.e., $\tilde{U}(az) = a^n \tilde{U}(z)$. Direct integration of Eq. (17) yields

$$\begin{aligned} \langle \delta n_R \rangle \Big|_{\tau \rightarrow \infty} &\simeq f_0''(v_A) \sqrt{\frac{2}{m_i^3}} \sqrt{|U(z)|} \left[\frac{n}{n+2} \right. \\ &\quad \left. \times (|U_m| - |U(z)|) - \frac{2}{3(n+2)} |U(z)| \right]. \quad (19) \end{aligned}$$

Note that the term $\propto f_0'(v_A)$ vanishes identically, hence the damping is absent. Since $\langle \hat{\mathcal{K}} \rangle \langle \hat{\mathcal{K}} \rangle \neq \hat{\mathcal{K}}\hat{\mathcal{K}} = -1$, we can only estimate the coupling constant to be $\chi \sim f_0''(v_A) [v_A^3/n_0] \sqrt{2/m_i^3}$. The index n is formally not defined for an arbitrary potential, but it can be estimated numerically, given the wave profile [10].

Clearly, in the asymptotic limit, $\tau \gg \tau_{tr}$, the damping rate vanishes due to phase mixing. Nevertheless, the resonant particles still contribute the wave dynamics, in that

$$\langle \delta n_R \rangle \sim f_0''(v_A) |b|^3, \quad (20)$$

thus determining a new nonlinear wave equation.

Simple Bernstein-Green-Kruskal type analysis shows that the ‘height’ of the asymptotic plateau on the PDF depends on the plasma parameters through m_1 and m_2 [10]. The difference between the plateau and the initial, Maxwellian PDF evaluated at v_A is

$$f_{\text{plat}} - f_{\text{Maxw}}|_{v_A} = \frac{m_1 |b|}{m_2 v_A}. \quad (21)$$

Thus we conclude that there is under-population of trapped particles (void on the PDF, $f_{\text{plat}} < f_{\text{Maxw}}$) at low β 's and over-population (bump, $f_{\text{plat}} > f_{\text{Maxw}}$) at high β 's.

Finally, assuming weak damping of a nonlinear Alfvén wave (e.g., ion-cyclotron damping), one can see [10] from the conservation of the parallel adiabatic invariant $J = \oint p_{\parallel} dz$ that trapped particles will condense near the bottom of the wave potential: $\Delta v_{\parallel} \propto |b|$, forming a clump on the PDF at $v \simeq v_A$.

VI. ACKNOWLEDGMENTS

It is a pleasure to thank Patrick Diamond, Valentin Shevchenko, Marshall Rosenbluth, and Vitaly Galinsky for valuable contributions to this work. We also thank Roald Sagdeev, Shadia Habbal, Vitaly Shapiro, Ramesh Narayan, Eliot Quataert, and Sally Ride for interesting discussions.

-
- [1] R.P. Lepping and K.W. Behannon, *J. Geophys. Res.* **91**, 8725 (1986).
 - [2] M. Neugebauer, *Geophys. Res. Lett.* **16**, 1261 (1989).
 - [3] B.T. Tsurutani, C.M. Ho, J.K. Arballo, E.J. Smith, B.E. Goldstein, M. Neugebauer, A. Balogh, and W.C. Feldman, *J. Geophys. Res.* **101**, 11027 (1996).
 - [4] M.V. Medvedev, P.H. Diamond, V.I. Shevchenko, and V.L. Galinsky, *Phys. Rev. Lett.* **78**, 4934 (1997).
 - [5] M.V. Medvedev and P.H. Diamond, *Phys. Plasmas* **3** 863 (1996).
 - [6] M.V. Medvedev, V.I. Shevchenko, P.H. Diamond, and V.L. Galinsky, *Phys. Plasmas*, **4** 1257 (1997).
 - [7] B.J. Vasquez and P.G. Cargill, *J. Geophys. Res.* **98**, 1277 (1993).
 - [8] B.J. Vasquez and J.V. Hollweg, *J. Geophys. Res.* **101**, 13,527 (1996).
 - [9] M.V. Medvedev and P.H. Diamond, *Phys. Rev. E* **56**, R2371 (1997).
 - [10] M.V. Medvedev, P.H. Diamond, M.N. Rosenbluth, and V.I. Shevchenko, *Phys. Rev. Lett.* **81**, 5824 (1998).

- [11] R.H. Cohen and R.M. Kulsrud, *Phys. Fluids* **17**, 2215 (1974).
- [12] C.F. Kennel, B. Buti, T.Hada, and R. Pellat, *Phys. Fluids* **30**, 1949 (1988).
- [13] D.J. Kaup and A.C. Newell, *J. Math. Phys.* **19**, 798 (1978).
- [14] A. Rogister, *Phys. Fluids* **14**, 2733 (1971).
- [15] E. Mjølhus and J. Wyller, *J. Plasma Phys.* **40**, 299 (1988).
- [16] S.R. Spangler, *Phys. Fluids B* **1**, 1738 (1989).
- [17] S.R. Spangler, *Phys. Fluids B* **2**, 407 (1989).
- [18] G.W. Hammett and F.W. Perkins, *Phys. Rev. Lett.* **64**, 3019 (1990).
- [19] M.A. Malkov, R.Z. Sagdeev, and V.D. Shapiro, *Phys. Lett. A* **151**, 505 (1990).
- [20] M.A. Malkov, C.F. Kennel, C.C. Wu, R. Pellat, and V.D. Shapiro, *Phys. Fluids B* **3**, 1407 (1991).
- [21] B.T. Tsurutani and E.J. Smith, *Geophys. Res. Lett.* **13**, 263 (1986).
- [22] V.D. Shapiro, *Sov. Phys. JETP* **17**, 416 (1963).
- [23] T.M. O’Neil, *Phys. Fluids* **8**, 2255 (1965).
- [24] E. Mjølhus and J. Wyller, *Phys. Scr.* **33**, 442 (1986).

FIG. 1. Wave profile evolution of a linearly polarized wave with a sinusoidal initial profile propagating parallel to the magnetic field for $T_e \simeq T_i$ and $\beta = 0$ (a) and $\beta = 1$ (b).

FIG. 2. The coefficients $M_1 = 2m_1$ and $M_2 = 2m_2$ vs. $1/\beta$ for $T_e = T_i$.

FIG. 3. The arc-type rotational discontinuity propagating obliquely to the magnetic field, $\Theta \sim 30^\circ$, with $\Delta\phi < \pi$, (a) - amplitude and phase profiles, (b) - hodograph.

FIG. 4. Same as Fig. 3 for the S-type directional discontinuity propagating parallel to the field.

FIG. 5. Wave energy evolution.

FIG. 6. The β - T_e/T_i -diagram of state. The region inside the curve corresponds to highly damped turbulence. No steep fronts appear. There are steep fronts in the region outside the curve.

FIG. 7. Trapping potential.

NOTE TO EDITOR:
ALL FIGURES SHOULD BE SCALED TO THE SINGLE COLUMN FORMAT.

Fig. 1:

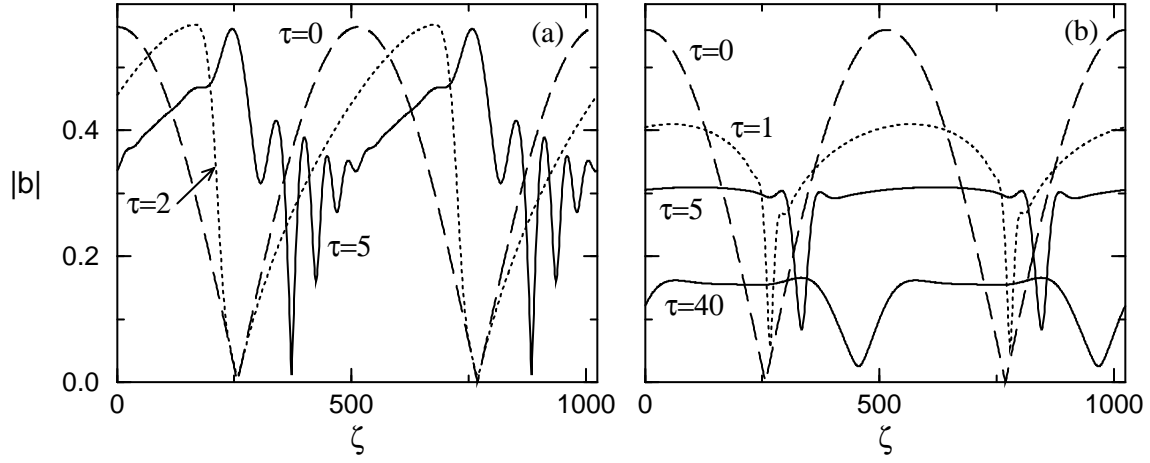
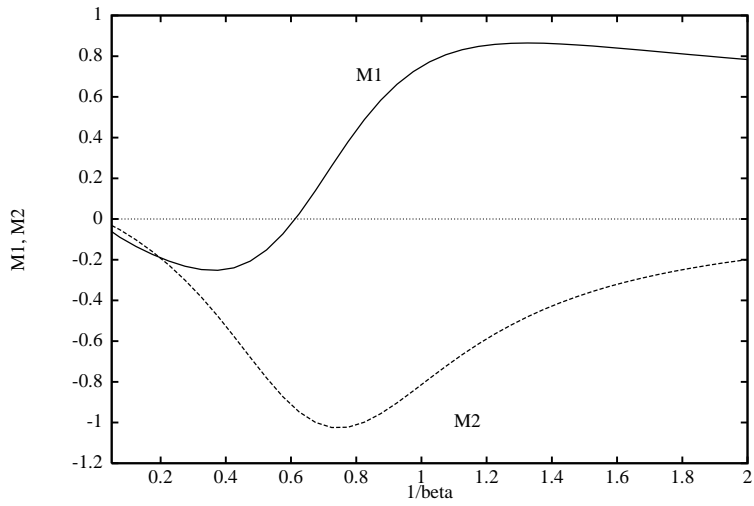


Fig. 2:



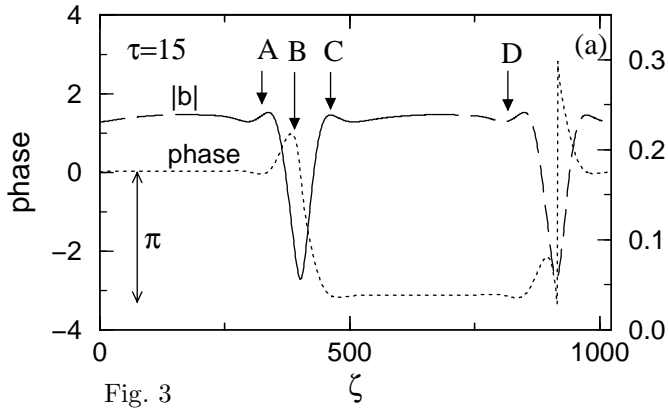


Fig. 3

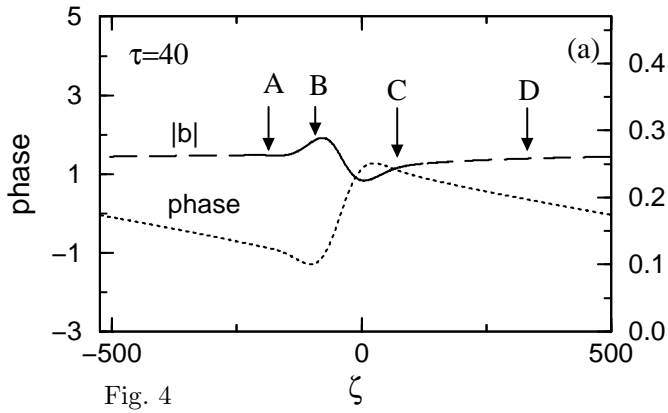
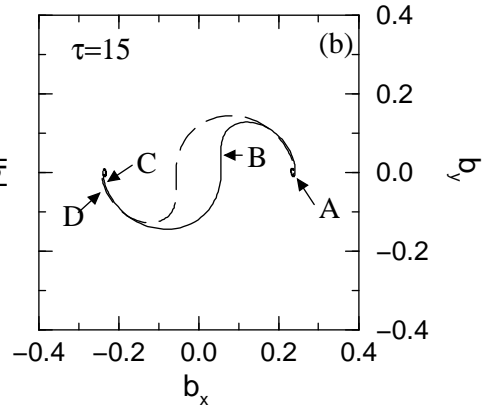


Fig. 4

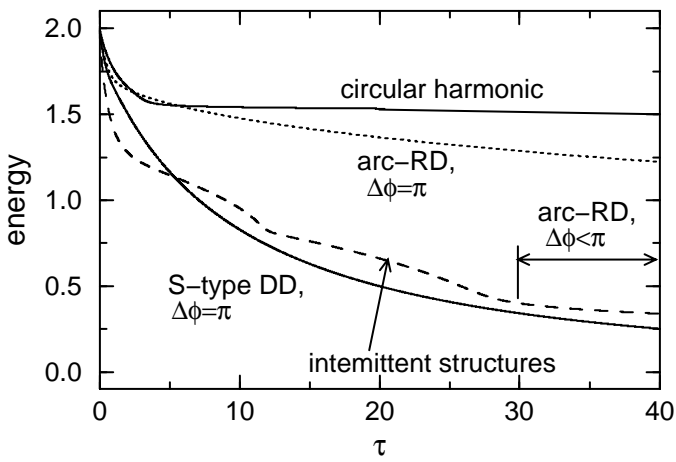
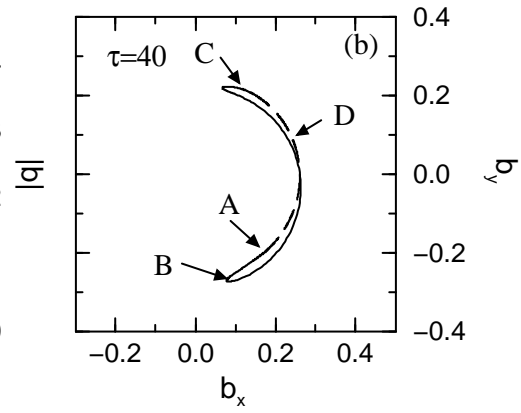


Fig. 5

Fig. 6:

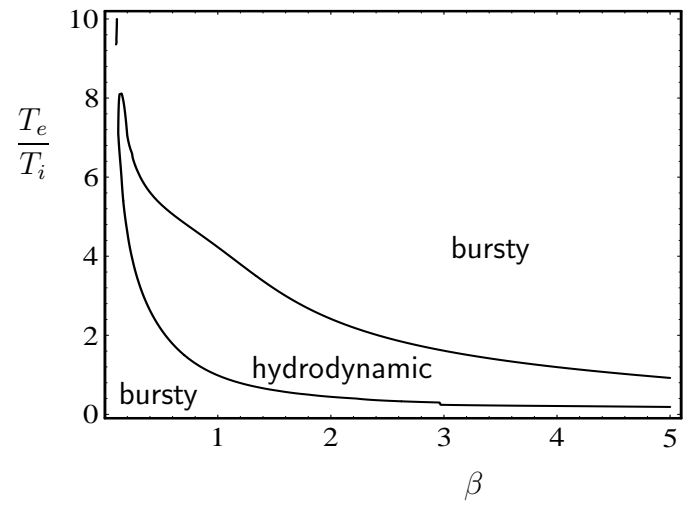


Fig. 7:

